Blood Pressure Simulator using An Optimal Controller with Disturbance Observer

Cheol-Han Kim, Gi-Bong Han, Hyun-Chul Lee, Yun-Jin Kim, Ki-Gon Nam, Geon Sa-Gong, Young-Jin Lee, Kwon-Soon Lee, Gye-Rok Jeon, and Soo-Young Ye*

Abstract: The various blood pressure simulators have been proposed to evaluate and improve the performance of the automatic sphygmomanometer. These have some problems such as the deviation of the actual blood pressure waveform, limitation in the blood pressure condition of the simulator, or difficulty in displaying the blood flow. An improved simulator using disturbance observer is proposed to supplement the current problems of the blood pressure simulator. The proposed simulator has an artificial arm model capable of feeding appropriate fluids that can generate the blood pressure waveform to evaluate the automatic sphygmomanometer. A controller was designed and thereafter, simulation was performed to control the output signal with respect to the reference input in the fluid dynamic model using the proposed proportional control valve. To minimize the external fluctuation of pressure applied to the artificial arm, a disturbance observer was designed on the plant. A hybrid controller combined with a proportional controller and feed-forward controller was fabricated after applying a disturbance observer to the control plant. Comparison of the simulations between the conventional proportional controller and the proposed hybrid controller indicated that even though the former showed good control performance without disturbance, it was affected by the disturbance signal induced by the cuff. The latter exhibited an excellent performance under both situations.

Keywords: Automatic sphygmomanometer, blood pressure simulator, disturbance observer, hybrid controller, non-invasive method, oscillometric, proportional controller.

1. INTRODUCTION

Blood pressure measurement is a standard and necessary practice in evaluating the health condition of patients in a clinical field. The accuracy of the measurement is crucial for controlling a patient's condition in the case of acute patients having hypertension or undergoing surgical operation [1]. Therefore, automatic sphygmomanometers that can be used by the patient for simplicity in the measuring of blood pressure have been widely utilized in homes as well as hospitals and clinics.

The measuring methods of blood pressure may largely be classified into the categories of invasive and non-invasive; non-invasive measuring methods include auscultation method, palpation, ultrasonic wave method, and oscillometric method [2-4]. Among them, the oscillometric method has been generally used in the automatic sphygmomanometer due to its convenience in use. In case of the automatic sphygmomanometer adopting the oscillometric method, the blood pressure measured by means of the oscillometric method should be compared with that measured by the invasive method to improve the accuracy of the instrument system. As the invasive method requires the inconvenience of surgical operation, the non-invasive blood-pressure simulation system has been broadly used [5].

Manuscript received July 1, 2006; revised August 2, 2007; accepted October 4, 2007. Recommended by Editorial Board member Sun Kook Yoo under the direction of Editor Jin Young Choi. This work was supported by the Health Medical Technology Research of the Ministry of Health and Welfare (02-PJ3-PG6-EV05-0001).

Cheol-Han Kim and Ki-Gon Nam are with the School of Electronics Engineering, Pusan National University, Busan, Korea (e-mails: sensor2207@hanamil.net, kgnam@ pusan.ac.kr).

Gi-Bong Han is with the Dept. of Electronics Engineering, Ulsan University, Ulsan, Korea (e-mail: kbhan62@ empal.com).

Hyun-Chul Lee is with Doowon Technical College, Anseong-si, Gyeoggi-do, Korea (e-mail: hclee@doowon.ac.kr).

Yun-Jin Kim is with the Dept. of Family Medicine, College of Medicine, Pusan National University, Ami-dong, Seo-gu, Busan, Korea (e-mail: yjkim@pusan.ac.kr).

Kwon-Soon Lee and Geon Sa-Gong are with the Dept. of Electrical Engineering, Dong-A University, Busan, Korea (e-mails: kslee@daunet.donga.ac.kr, gsagong@donga.ac.kr).

Young-Jin Lee is with the Dept. of Electrical and Instrument Control, Korea Aviation Polytechnic College, Sachun, Kyungnam, Korea (e-mail: airlee011@hanmail.net).

Gye-Rok Jeon is with the Dept. of Biomedical Engineering, College of Medicine, Pusan National University, 33-5, Seo-gu, Bumin-dong 3-ga, Busan, Korea (e-mail: grjeon@pusan.ac.kr).

Soo Young Ye is with the BK21 Medical Science Education Center, School of Medicine, Pusan National University, Bumin-dong 3-ga, Busan, Korea (e-mail: syye@pusan.ac.kr).

* Corresponding author.

However, in case of the current blood pressure simulator, the pulse waveform of pressure produced in the automatic sphygmomanometer differs from the actual pulse type waveform pulse wave produced in the human body. Furthermore, the conventional blood pressure simulator cannot be applied because it produces pressure by applying air pressure in the cuffs. There is the disadvantage of limitation in pressure condition that can be applied in the assessment of the automatic sphygmomanometer, and the blood flow in the blood vessel cannot be reproduced [6]. In general, it is very difficult to reproduce the blood pressure waveform belonging to the low pressure range using the pressure flowing fluid in low pressure tubes such as the blood pressure in the blood vessels. A new type of fluid circulation blood pressure simulator is proposed in this study to supplement problems of the conventional blood pressure simulator used in development and evaluation of the automatic sphygmomanometers.

Various pressure waveforms of fluid flowing into the tube in the proposed blood pressure simulator were reproduced by operating the proportional control valve after applying pressure on the fluid in the pressurized oil tank. After that, appropriate fluid was supplied by operating the proportional control valve, which enabled the replication of various pressure waves of the fluid flowing in the tube. To accomplish this work, the mathematical model was carefully reviewed in cooperating with the proposed blood pressure simulator. After modeling the driving signal as the input signal and the pressure in the internal pipe as the output signal, the simulation on system parameters such as internal volume, cross-section of orifice and supply pressure, which are sensitive to dynamic characteristics of the system, was accomplished. System parameters affecting the dynamic characteristic were analyzed in the frequency bandwidth and also reflected in the design of the plant. The performance evaluator of fluid dynamic characteristic using proportional control signal was fabricated on the basis of obtained simulation result. An experimental apparatus was set-up and measurements on the dynamic characteristic, nonlinearity, and rising and falling response were carried out to verify the characteristic of the fluid dynamic model.

A controller was designed and thereafter, simulation was performed to control the output signal with respect to the reference input in the fluid dynamic model using the proposed proportional control valve. To minimize the external fluctuation of pressure applied to the artificial arm, a disturbance observer was designed on the plant to be controlled. A hybrid controller combined with a proportional controller and feed-forward controller was fabricated after applying a disturbance observer to the control plant. Comparison of the simulations between the conventional proportional controller and the proposed hybrid simulator indicated that even though the former showed good control performance without disturbance, it was seriously affected by the pressure induced by the cuff. However, the latter exhibited an excellent performance under both situations.

2. CONSTITUTION OF THE BLOOD PRESSURE SIMULATOR AND DYNAMIC CHARACTERISTICS OF THE SYSTEM

2.1. Constitution of the blood pressure simulator

The blood pressure simulator is fabricated to reproduce the pressure wave of fluids flowing in the tubes. Fig. 1 shows the schematic diagram of the blood pressure simulator. First of all, the oil is sent to the pressure tank using a circulation pump and then pressure is applied to the oil gathered in the pressure tank using a compressor. At this point, an accumulator was used to alleviate the impact pressure produced in the compressor.

The pressurized oil in the pressure tank flows into the tubes through the proportional control valve. The proportional control valve produces the pressure wave of fluids flowing in the tube by opening and closing of the valve. Also, the pressure of fluid produced by the proportional valve produces pressure in the fluid flowing in the tube of the artificial human arm manufactured with silicon, which is connected in parallel with the pipe. The fluid flows through a thin tube connected to the end of the pipe and then is stored in the fluid tank.

The pressure wave is formed using a personal computer to reproduce the pressure generated in the artificial silicon arm. The pressure of the fluid flowing in the artificial arm is reproduced like the blood pressure produced in the human arm, by inputting the obtained pressure wave into the controller and then controlling the tube pressure.

2.2. System dynamics

The electric pressure servo devices include a series of devices that control fluid pressure or the amount of flow under input of electric command signals [7], and the pressure of fluid flowing in the tubes is controlled

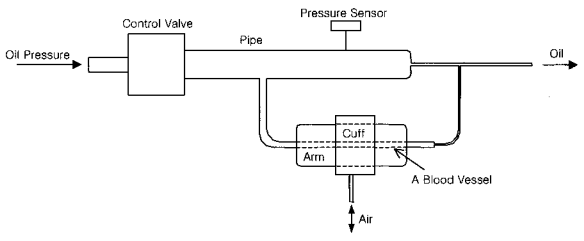

Fig. 1. A schematic diagram of the blood pressure simulator.

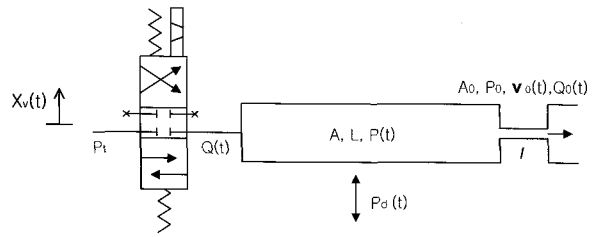

Fig. 2. Block diagram of electro-hydraulic servo system.

by these devices in this study. The block diagram of the electro-hydraulic servo system is presented in Fig. 2.

Proportional control valve may model as the first system as shown below:

$$T_{sv}\frac{dx_v(t)}{dt}+x_v(t)=K_{sv}K_a v(t), \tag{1}$$

where T_{sv}, $x_v(t)$, K_{sv}, K_a, and $v(t)$ indicate time constant of each valve, displacement of spool, valve gain, valve amplifier gain, and control input respectively. The amount of flowing between the proportional control valve and pipe may be expressed as follows:

$$Q(t)=C_d W_d x_v(t)\sqrt{\frac{2g(p_t-p(t)-p_d(t))}{\gamma}}, \tag{2}$$

where C_d, W_d, P_t, $P(t)$, $P_d(t)$, and ρ indicate discharge coefficient, valve area gradient, supplied pressure, pressure in the pipe, fluctuation pressure, and fluid density respectively. In considering the compressibility of the moving fluid, the continuity equation of fluid in the pipe may be expressed as follows:

$$Q(t)=v_o(t)A_o+\frac{AL}{\beta}\frac{d(P(t)+P_d(t))}{dt}, \tag{3}$$

where A_o, $v_o(t)$, A, L, and β indicate the section area of orifice attached at the ends of each pipe, flow rate of fluid in orifice, section area of tube, length of tube, and bulk coefficient respectively. When the orifices attached at the ends of the pipes are assumed to be chalk-type orifices, the quantity of flow of output, $Q_o(t)=v_o(t)A_o$, may be expressed as follows [8]:

$$Q(t)=\frac{A_o^2 g\{P(t)+P_d(t)-P_o\}}{8\pi\nu\gamma l}, \tag{4}$$

where Q_o, P_o, l, γ, ν, and g indicate the quantity of flow at orifice, atmospheric pressure, length of the chalk of orifice, dynamic viscosity coefficient of fluid, specific gravity of oil, and the acceleration of gravity respectively.

When (2), (3), and (4) are arranged, continuity equation of the fluid is expressed as follows:

$$\begin{aligned}&\frac{AL}{\beta}\frac{d\{P(t)+P_d(t)\}}{dt}\\&=C_d W_d x_v(t)\sqrt{\frac{2g\{P_t-P(t)-P_d(t)\}}{\gamma}}\\&\quad-\frac{A_o^2 g\{P(t)+P_d(t)-P_o\}}{8\pi\nu\gamma l},\end{aligned} \tag{5}$$

where $x_v(t)$ and $P(t)$ are status variables and $v(t)$ is control input. $P_d(t)$ acts as the disturbance influencing on the pressure in the tube.

Equations (1) and (5) may be expressed as state space equation and is shown below:

$$\dot{X}_p(t)=A_p X_p(t)+B_p U(t)+L_p d(t), \tag{6}$$

$$Y_p(t)=C_p X_p(t), \tag{7}$$

where A_p, B_p, C_p, and L_p are as follows:

$$\begin{aligned}A_p&=\begin{vmatrix}-\frac{1}{T_{sv}} & 0\\ \frac{C_d W_d \beta}{AL}\sqrt{\frac{2\gamma P_t}{g}} & -\frac{A_o^2 g\beta}{8\pi\nu\gamma lAL}\end{vmatrix},\\ B_p&=\begin{vmatrix}\frac{K_v K_a}{T_{sv}}\\ 0\end{vmatrix},\quad C_p=\begin{bmatrix}0 & 0.1\end{bmatrix},\\ L_p&=\begin{vmatrix}0\\ \frac{dP_d(t)}{dt}-\frac{A_o^2 g\beta}{8\pi\nu\gamma lAL}P_d(t)\end{vmatrix},\end{aligned} \tag{8}$$

where L_p is the disturbance item that influences on the controlling of pressure in the tube.

As indicated above, the blood pressure simulator is mathematically modeled. The system parameter that determines the dynamic characteristics of the blood pressure simulator can be chosen diversely according to purpose. The relationship between the pressures supplied into the tube is identified through the internal volume of the tube, section area of tube outlet, and proportional control valve, and system parameters are decided on the basis of these results.

3. DESIGN OF CONTROLLER

To control the pressure wave of fluid flowing in the tubes with disturbance, the disturbance monitor is designed on the plant and the optimum controller for this whole system is also designed. Fig. 3 shows the

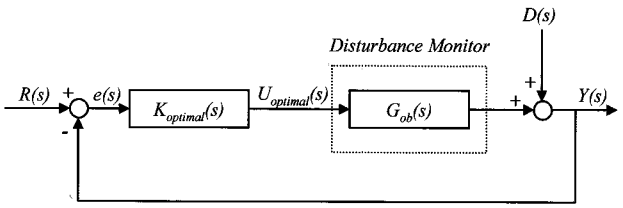

Fig. 3. The block diagram of optimal controller with disturbance observer.

block-line drawing of the optimum controller with disturbance observer.

In Fig. 3, $R(s)$, $e(s)$, $U_{optimal}(s)$, $D(s)$, and $Y(s)$ mean standard input, error signal, feedback control input, disturbance, and output, respectively. Also, $K_{optimal}(s)$ and $G_{ob}(s)$ signify transfer functions of the feedback controller and the actual plant with mounted disturbance monitor.

The mixed controller should be designed through design of the disturbance observer and design of the feedback controller.

3.1. Disturbance observer

The disturbance monitor was originally suggested by Ohishi. With application of this device, the actual plant with mounted disturbance monitor displays the same dynamic characteristics as the nominal model used in designing of the disturbance monitor. It is commonly utilized in various fields for the purpose of robust control and disturbance removal [9-11].

Fig. 4 indicates the actual plant with amounted disturbance monitor. Where, $U_{optimal}(s)$, $w(s)$, and $Y(s)$ indicate control input of optimal controller, control input including disturbance observer, and output, respectively; and $v(s)$ shows the observed disturbance signal.

Futhermore, $G_n(s)$, $\Delta G(s)$, and $Q(s)$ signify nominal model of plant, additive model error, and Q-filter respectively. System output, $Y(s)$ may be expressed as follows:

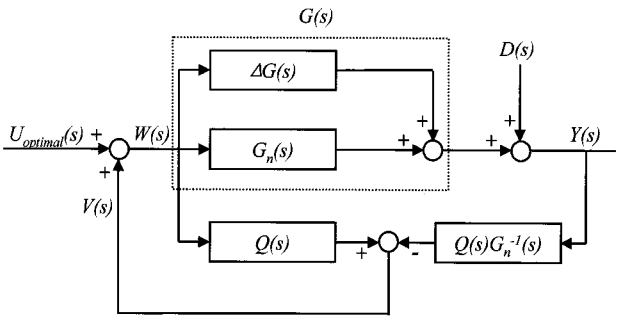

Fig. 4. The proposed schematic diagram of disturbance observer.

$$Y(s)=\frac{\{G_n(s)+\Delta G(s)\}G_n(s)}{G_n(s)+\Delta G(s)Q(s)}u(s)+\frac{\{1-Q(s)\}G_n(s)}{G_n(s)+\Delta G(s)Q(s)}D(s), \tag{9}$$

where the transfer function, $G_u(s)$, to control input, $U_{optimal}(s)$, is

$$G_u(s)=\frac{\{G_n(s)+\Delta G(s)\}G_n(s)}{G_n(s)+\Delta G(s)Q(s)} \tag{10}$$

and the transfer function, $G_d(s)$, to disturbance, $D(s)$, is

$$G_d(s)=\frac{\{1-Q(s)\}G_n(s)}{G_n(s)+\Delta G(s)Q(s)}. \tag{11}$$

Also, Q-filter is the filter for passage of low frequency and is designed as described below.

In nodal point frequency area,

$$Q(s)\approx 1 \tag{12}$$

not lower than the frequency in nodal point,

$$Q(s)\approx 0. \tag{13}$$

When Q(s)-filter is designed to have the characteristics of (12) and (13), and when it is applied to (10) and (11), the transfer functions to control input, $U_{optimal}(s)$, and disturbance, $D(s)$, are as follows respectively:

$$G_u(s)\approx G_n(s), \tag{14}$$

$$G_d(s)\approx 0, \tag{15}$$

where the actual plant with mounted disturbance monitor is the nominal model, $G_n(s)$, used in the design of the disturbance monitor, it can be known that disturbance is completely removed because the robust to modeling error, $\Delta G(s)$, and the transfer function, $G_d(s)$, to disturbance are zero.

3.2. Design of optimal controller

It can be found that the plant's transfer functions, $G_{ob}(s)$, is $G_n(s)$ when disturbance monitor is mounted. Therefore, Fig. 4 may be expressed as shown in Fig. 5.

When $G_n(s)$ is converted into state equation form to design optimal controller, it may be expressed as follows:

$$\dot{X}_n(t)=A_nX_n(t)+B_nu_{optimal}(t), \tag{16}$$

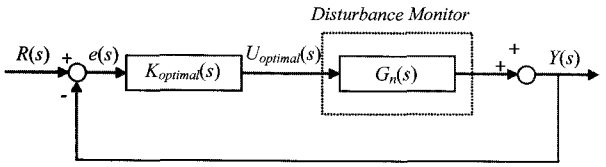

Fig. 5. The block diagram of optimal controller.

$$y_n(t) = C_n x(t). \tag{17}$$

In (16) and (17), control input, $u_{optimal}(t)$, is as follows:

$$u_{optimal}(t) = K_{optimal}(s)e(s). \tag{18}$$

In (18), $K_{optimal}(t)$ may be expressed as follows:

$$K_{optimal}(t) = G(sI - A_n + B_n G + HC_n)^{-1} H. \tag{19}$$

In (19), Kalman filter gain matrix, H, may be expressed as follows:

$$H = \frac{1}{\mu} PC_n^T, \tag{20}$$

where matrix P may be obtained with use of the 'Filter Algebraic Riccati Equation'.

$$A_n P + PA_n^T + LL^T - \frac{1}{\mu} PC_n^T C_n^T P = 0 \tag{21}$$

In (21), μ and L are design variables. Now, to select the design variables μ and L, the equation below is used.

$$G_f(s) = \frac{1}{\sqrt{\mu}} C_n (sI - A_n)^{-1} L, \tag{22}$$

where L is the $K_{optimal}(s)$ in Fig. 3, Fig. 5 in (22), and is expressed as shown below:

$$L = C_n (C_n C_n^T)^{-1}.$$

And μ becomes 0.06 by nodal point frequency.

Gain matrix, G, in equation (20) is as follows:

$$G = \frac{1}{\rho} B_n^T S. \tag{23}$$

In (23), when S may be obtained with use of the below shown 'Algebraic Riccati Equation' in the condition of $\rho \to 0$.

$$SA_n + A_n^T S + C_n^T C_n - \frac{1}{\rho} SBB^T S = 0 \tag{24}$$

In (24), $\rho = 1 \times 10^{-9}$.

4. RESULT AND DISCUSSION

A simulator was implemented to reproduce the blood pressure in the blood vessel. Table 1 shows the specifications of the control valve, plant, and fluid. It is attempted to identify the influence of internal volume of the tube, section area of the orifice, and supplied pressure, which are sensitive to the dynamic characteristics of the whole system. Two system parameters among the internal volume of the tube, section area of the orifice, and supplied pressure were fixed, based on the 2nd specification of Table 2. Thereafter, simulation was carried out while changing the one remaining system parameter. A controller based on this result was designed.

Fig. 6 indicates the frequency characteristic when internal volume of tube, $A \times L$, and section area of orifice, A_o are fixed to 353.4cm^3 and 0.14cm^2 respectively and when supplied pressure is changed to 30kgf/cm^2, 3kgf/cm^2, and 1kgf/cm^2 respectively. As shown in Fig. 6, it can be found that DC gain and bandwidth increase with increasing supplied pressure, P_t.

Fig. 7 shows the frequency characteristic when internal volume of the tube, $A \times L$ and supplied pressure, P_t are fixed to 353.4cm^3 and 3kgf/cm^2 respectively and when section area of the orifice

Table 1. The specification of plant.

Items	Specifications
Valve time constant (T_{sv})	1/20
Valve gain (K_{st})	10V/cm
Valve amplifier gain (K_a)	100
Output coefficient (C_d)	0.7
Valve area gradient (W_d)	0.83
Bulk coefficient of fluid (β)	7033kg/cm^2
Dynamic viscosity coefficient (ν)	80mm^2/s
Specific gravity (γ)	0.82
Internal volume of tube ($A \times L$)	353.4cm^2
Length of orifice (l)	2cm
Section area of orifice (A_o)	0.14cm
Supplied pressure (P_t)	3kgf/cm^2

Table 2. The specification of plant used for simulation.

	Internal olume of tube ($A \times L$)	Section area of orifice (A_o)	Supplied pressure (P_t)
1	100cm^3	0.1cm^2	30kgf/cm^2
2	353.4cm^3	0.14cm^2	3kgf/cm^2
3	600cm^3	0.3cm^2	1kgf/cm^2

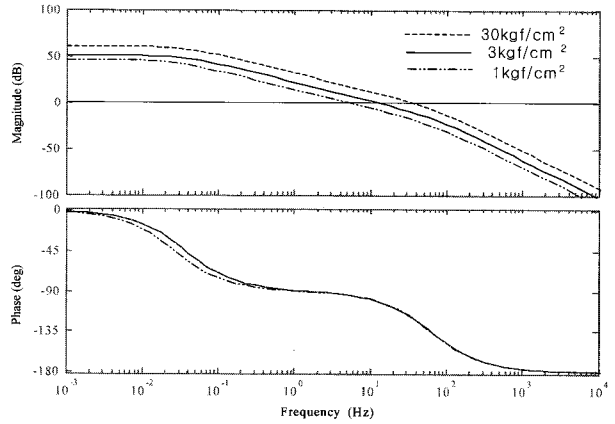

Fig. 6. The bode plot of plant according to supplied pressure.

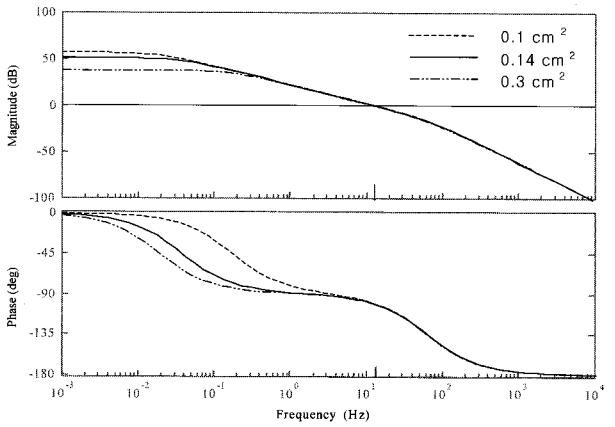

Fig. 7. The bode plot of plant according to the section area of orifice.

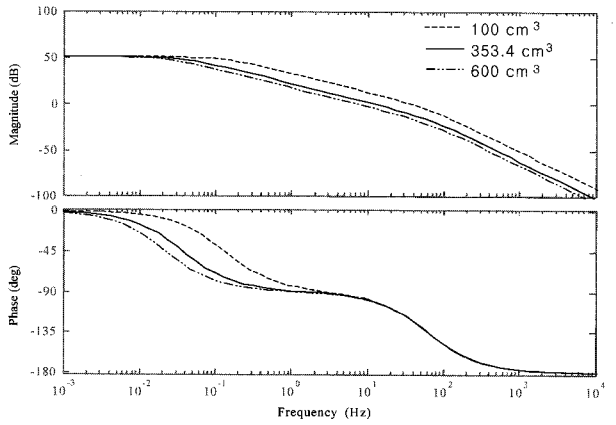

Fig. 8. The bode plot of plant according to the internal volume of the tube.

increases to 0.1cm^2, 0.14cm^2, and 0.3cm^2 respectively. It is apparent that DC gain increases when the section area of orifice, A_o is reduced, regardless of bandwidth.

Fig. 8 displays the frequency characteristic when supplied pressure, P_t and section area of orifice, A_o are fixed to 3kgf/cm^2 and 0.14cm^2, respectively and when the internal volume of the tube is changed to

Table 3. The mathematical equation of low pass filter and disturbance, and reference blood pressure.

Kinds	Functions
Lowpass filter	$Q(s) = \dfrac{0.09s+1}{1\times10^{-6}s^3+9\times10^{-4}s^2+9\times10^{-2}+1}$
Disturbance	$P_d(t) = 100+10\sin(4\pi t) + 40\pi\cos(4\pi t)$
Reference blood pressure	$P_r(t) = 21.82\cos(2\pi t-2.41) + 6.24\cos(4\pi t+2.65) + 3.59\cos(6\pi t+1.27) + 2.04\cos(8\pi t-1.37) + 1.42\cos(10\pi t+2.31)$

100cm^3 and 353.4cm^3, and 600cm^3, respectively. It can be found that bandwidth increases when the internal volume of tube, $A\times L$, decreases, regardless of DC gain.

Table 3 indicates the mathematical equations expressing the disturbance and the human blood pressure transmitted from lowpass filter and cuff designed based on the plant.

Fig. 9 shows the pressure signal transmitted from the cuff to the blood vessels. If the pressure to the cuff induced by the automatic sphygmomanometer is assumed to be $100+10\sin(4\pi t)$, the pressure signal transmitted to the blood vessels may be expressed as follows:

$$P_d(t) = 100+10\sin(4\pi t)+40\pi\cos(4\pi t).$$

Fig. 10 indicates the reference input signal for the evaluation of the dynamic characteristic of the blood pressure simulator. Fig. 11 shows the bode plot of the feedback control system with and without disturbance observer. Fig. 12 displays the control performance of the feedback control system with and without disturbance observer regarding to reference input without disturbance signal, where it can be found that the performances of optimal controller with disturbance observer and optimal controller are favorable.

Fig. 13 presents the control performance of optimal controller with disturbance observer and optimal controller pertaining to reference input with disturbance signal, which is transmitted from the cuff to the interior of tube. Where, it can be found that the performances of optimal controller with disturbance observer are favorable but the performance of optimal controller is significantly influenced by the disturbance signal transmitted from the cuff.

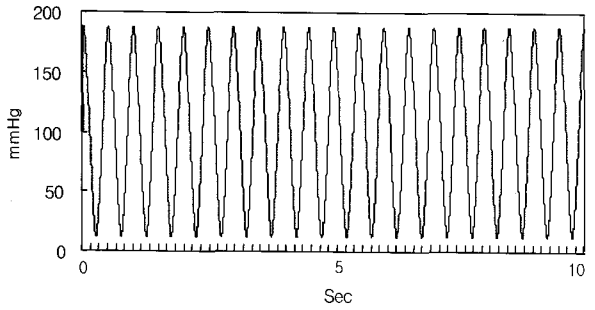

Fig. 9. The pressure signal transmitted from the cuff to the blood vessel.

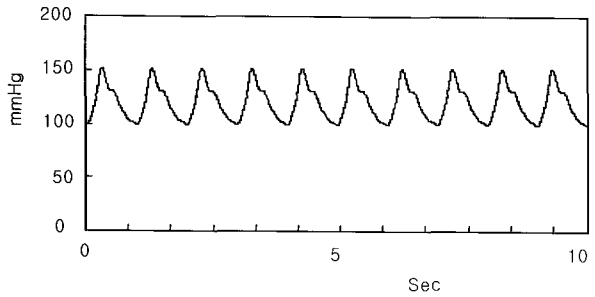

Fig. 10. The reference input signal for the evaluation of the dynamic characteristic of the blood pressure simulator.

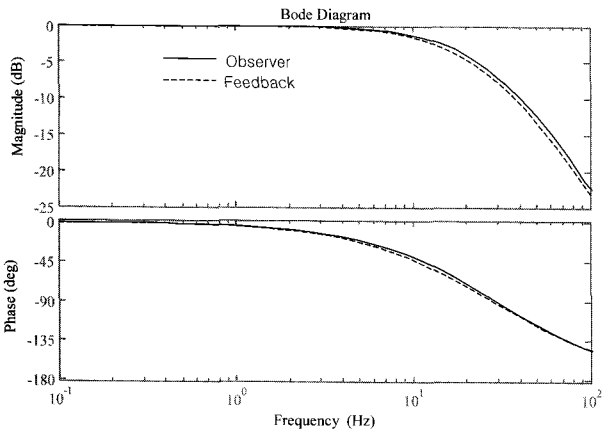

Fig. 11. The bode plot of feedback control system with and without disturbance observer.

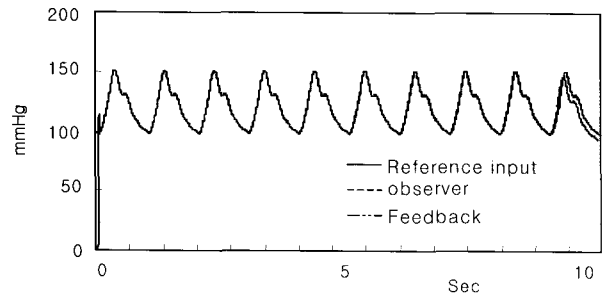

Fig. 12. The control performance of control feedback system with and without disturbance observer regarding to reference input without disturbance signal.

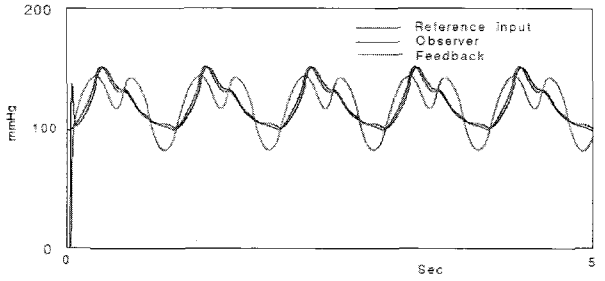

Fig. 13. The control performance of feedback control system with and without disturbance observer regarding to reference input with disturbance signal.

Experimental results indicate that supplied pressure has influence on DC gain and bandwidth of system, and also that the change in the internal volume of tube has influence on bandwidth regardless of DC gain. However, the change in the section area of the orifice has influence on DC gain regardless of bandwidth. It can be found that the traditional optimal controller shows favorable control performance when without disturbance signal but, when disturbance signal is transmitted from the cuff to the interior of the tube, significant influence is expressed, and furthermore that optimal controller with disturbance observer exhibits an excellent control performance and disturbance removal performance regardless of the disturbance signal transmitted from the cuff.

5. CONCLUSIONS

The characteristic of parameters that have influence on the system was identified in this study through modeling of the blood pressure simulator that reproduces the blood pressure wave in the blood vessels. As the result of simulation with application of the proposed controller, the following conclusions are obtained. (1) The characteristic of influence given by supplied pressure, internal volume of the tube, and the section area of orifices at outlet on replication of the blood pressure was identified and reflected in designing of the blood pressure simulators. (2) The optimal controller with disturbance observer shows excellent disturbance removal performance as well as excellent control performance while controlling the blood pressure simulator. (3) The traditional optimal controller shows favorable control performance when acting without the disturbance signal but is significantly influenced by the disturbance signal transmitted from the cuff into the interior of the tube.

REFERENCES

[1] J. K. Cheun, *Cardiopulmonary Physiology for the Clinicians*, Koon Ja Publishing Inc., 1996.

[2] G. M. Drzewiecki, J. Melbin, and A. Noordergraaf, "The Korotkoff sound," *Amm.*

Biomedical Eng., vol. 17, pp. 325-359, 1989.

[3] E. J. Marey, "Pression et vitesse du sang," *Physiologic Experimental*, Masson, Paris, Vol. 2, pp. 307-343, 1876.

[4] J. C. B. T. Morae and M. Cerulli, "A strategy for determination of systolic, mean and diastolic blood pressures from oscillonmetric pulse profiles," *Computer in Cardiology*, vol. 27, pp. 211-214, 2000.

[5] J. N. Amoore and W. B. Geake, "Evaluation of the critikon 8100 and spacelabs 90207 non-invasive blood pressure monitors using a test simulator," *J. Hum. Hypertens.*, vol. 11, no. 3, pp. 163-139, March 1997.

[6] K. G. Ng and C. F. Small, "Review of methods and simulators for evaluation of non-invasive blood pressure monitors," *J. Clin. Eng.*, vol. 17, pp. 469-479, 1992.

[7] J. S. Yun and H. S. Cho, "Application of an adaptive model following control technique to a hydraulic servo-system subjected to unknown disturbances," *Journal of Dynamic Systems Measurement and Control*, ASME, vol. 113, pp. 479-484, 1991.

[8] F. M. White, *Fluid Mechanics*, McGraw-Hill, Inc., 1979.

[9] T. Umeno and Y. Hori, "Robust speed control of DC servo motors using modern two degrees-of-Freedom controller design," *IEEE Trans. on Industrial Electronics*, vol. 8, no. 5, pp. 363-368, 1991.

[10] K. Yamada, S. Komada, M. Ishida, and T. Hori, "Characteristics of servo system using high order disturbance observor," *Proc. of IEEE Int. Conf. of Decision and Control*, pp. 3252-3257, 1996.

[11] E. Furutani M. Araki, S. Kan, T. Aung, H. Onodera, M.Imamura, G. Shirakami, and S. Maetani, "An automatic control system of the blood pressure of patients under surgical operation," *International Journal of Control, Automation, and System*, vol. 2, no. 1, pp. 39-54, 2004.

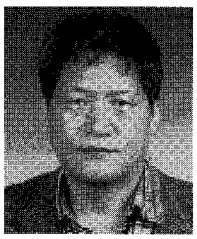

Choel-Han Kim received the B.S. degree from the Department of Physics, Pusan National University, Busan in 1984, the M.S. degree from the Department of Electrical Engineering, Dong-A University in 2001, and the Ph.D. degree in Electronic Engineering from Pusan National University. His current research interests include simulation and modeling.

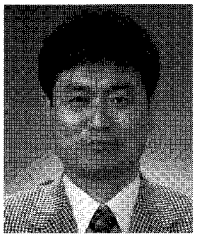

Gi-Bong Han received the B.S., M.S, and Ph.D. degrees in Mechanical Design Engineering from Pusan National University in 1986, 1992 and 1997, respectively. He was Senior Researcher at DAEWOO Electronics from 1994 until 2000. Currently, he is a Research Professor in the Department of Electrical Engineering, Ulsan University. His research interests include optimal control, adaptive control, and system identification.

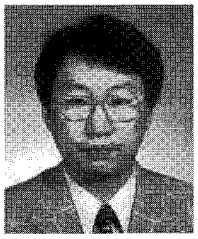

Hyun-Chul Lee is currently a Professor of Automobile Engineering at Doowon Technical College.

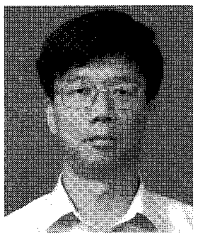

Yun-Jin Kim received the M.S. degree in the Department of Preventive Medicine from Yeonsei University in 1987. He received the Ph.D. degree in the Department of Parasitology in 1992 from the same institution. He is currently a Professor in the Department of Family Medicine at Pusan National University.

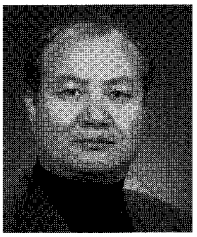

Ki-Gon Nam received the B.S. degree in Electronics Engineering from Pusan National University, Korea, in 1977, the M.S. degree in Electronics Engineering from Pusan National University, Korea, in 1981, and the Ph.D. degree in Electronics Engineering from Pusan National University in 1989. He was employed as a Senior Member of the research staff in the Dept. of Electrical & Computer Engineering. He is currently a Professor in the School of Electronics Engineering at Pusan National University. His research interests include computer vision, and pattern recognition.

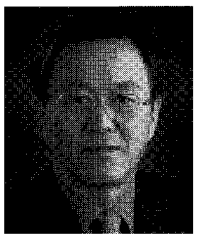

Geon Sa-Gong received the B.S. and M.S. degrees from the Department of Electronic Engineering, Pusan National University, Korea, in 1978 and 1981, respectively, and the Ph.D. degree from the Department of Electronic Engineering, Dong-A University, Busan, Korea, in 1993. Since 1985, he has been with the Department of Biomedical Engineering, College of Medicine, Pusan National University, Busan, Korea, where he is currently a Professor. His research interests are bio medical signal processing, modeling, and simulation.

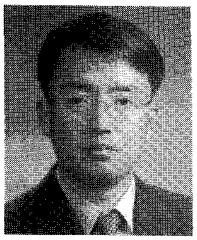

Young-Jin Lee received the B.S., M.S., and Ph.D. degrees in the Department of Electrical Engineering from Dong-A University, Busan, Korea, in 1992, 1994, and 2000, respectively. Since 2000, he has been with the Department of Electrical Instrument and Control at Korea Aviation Polytechnic College, where he is currently an Assistant Professor. His research interests are intelligent control, immune algorithm, and adaptive control.

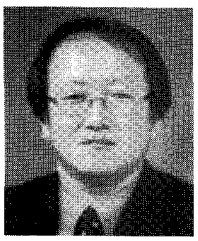

Kwon-Soon Lee received the B.S. degree from Chung Nam National University, Chung-nam, and the M.S. degree from the Department of Electrical Engineering from Seoul National University, Seoul, Korea, in 1973 and 1979, respectively. He received the Ph.D. from the Department of Electrical and Computer Engineering, Oregon State University, USA, in 1990. Since 1982, he has been with the Electrical, Electronic, and Computer Division, Dong-A University, Busan, Korea where he is currently a Professor. His recent research interests are intelligent control theory, immune algorithm, and application techniques for port automation systems, etc.

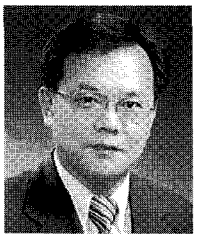

Gye-Rok Jeon received the B.S. and M.S degrees in Electronic Engineering from Pusan National University, Korea, in 1978 and 1981, and the Ph.D. in Electronic Engineering from Dong-A University, Pusan, Korea, in 1992. He is currently a Professor in the Department of Biomedical Engineering, College of Medicine, Pusan National University. His current research interests include simulation of blood pressure, biomedical signal processing, and ubiquitous health care.

Soo-Young Ye received the B.S. degree in Electronic Engineering from Dongseo University, Korea, in 1996, the M.S. degree in Electronic Engineering from Pusan National University in 1998, and the Ph.D. in Biomedical Engineering from Pusan National University in 2004. She is currently a Research Professor in the BK21 Medical Science Education Center, School of Medicine, Pusan National University. Her research interests include biomedical signal processing.